A Single-chain Antibody Conjugated to a Cage Amine Chelator and Labelled with Positron-Emitting Copper-64 for Diagnostic Imaging of Activated Platelets

Journal:	*Molecular Pharmaceutics*
Manuscript ID:	mp-2014-00209a.R1
Manuscript Type:	Article
Date Submitted by the Author:	n/a
Complete List of Authors:	Alt, Karen; Baker IDI, Paterson, Brett; University of Melbourne, Ardipradja, Katie; Baker IDI, Schieber, Christine; Bio21 Institute University of Melbourne, Buncic, Gojko; University of Melbourne, Lim, Bock; Baker IDI, Poniger, Stan; Departments of Nuclear Medicine and Centre for PET, Jakoby, Bjoern; Siemens Healthcare, Wang, Xiaowei; Baker IDI, O'Keefe, Graeme; Departments of Nuclear Medicine and Centre for PET, Tochon-Danguy, Henri; Departments of Nuclear Medicine and Centre for PET, Scott, Andrew; Ludwig Institute for Cancer Research, Melbourne Centre for Clinical Sciences Ackerman, Uwe; Nuclear medecine and centre for PET, PET chemistry Peter, Karlheinz; Baker IDI, Donnelly, Paul; University of Melbourne, School of Chemistry Hagemeyer, Christoph; Baker IDI Heart and Diabetes Institute , Vascular Biotechnology Laboratory

A Single-chain Antibody Conjugated to a Cage Amine Chelator and Labelled with Positron-Emitting Copper-64 for Diagnostic Imaging of Activated Platelets

Karen Alt[†1,2], Brett M. Paterson[†3], Katie Ardipradja[1,2,4,5], Christine Schieber[3], Gojko Buncic[3], Bock Lim[1,2], Stan S. Poniger[4], Bjoern Jakoby[6,7], Xiaowei Wang[2], Graeme J. O'Keefe[4,5], Henri J. Tochon-Danguy[4], Andrew M. Scott[4,5,8], Uwe Ackermann[4,5,8], Karlheinz Peter[†2,9], Paul S. Donnelly[†*3], Christoph E. Hagemeyer[†*1,10]

[1]Vascular Biotechnology Laboratory, Baker IDI, Melbourne, Australia.
[2]Atherothrombosis and Vascular Laboratory, Baker IDI, Melbourne, Australia.
[3]School of Chemistry and Bio21 Molecular Science and Biotechnology Institute, The University of Melbourne, Melbourne, Australia.
[4]Departments of Nuclear Medicine and Centre for PET, Austin Health, Melbourne, Australia.
[5]Department of Medicine, Dentistry and Health Sciences, The University of Melbourne, Melbourne, Australia.
[6]Siemens Healthcare, Erlangen, Germany.
[7]University of Surrey, Guildford, Surrey, United Kingdom.
[8]Ludwig Institute for Cancer Research, Austin Health, Melbourne, Australia.
[9]Central Clinical School, Monash University, Melbourne, Australia.
[10]School of Applied Sciences, RMIT University, Melbourne, Australia.
[†]Contributed equally

***Corresponding authors** Christoph E. Hagemeyer, PhD
Vascular Biotechnology Laboratory, Baker IDI Heart and Diabetes Institute
75 Commercial Road, Melbourne Victoria 3004, Australia
Phone: +61 3 8532 1494; Fax: +61 3 8532 110 e-mail: christoph.hagemeyer@bakeridi.edu.au
Paul S. Donnelly, PhD e-mail: pauld@unimelb.edu.au

Imaging of activated platelets using an activation specific anti GPIIb/IIIa integrin single-chain antibody ($scFv_{anti\text{-}LIBS}$) conjugated to a positron emitting copper-64 complex of a cage amine sarcophagine chelator (MeCOSar) is reported. This tracer was compared *in vitro* to a $^{64}Cu^{II}$ complex of the scFv conjugated to another commonly used macrocycle, DOTA. The $scFv_{anti\text{-}LIBS}$-MeCOSar conjugate was radiolabelled with $^{64}Cu^{II}$ rapidly under mild conditions and with higher specific activity than $scFv_{anti\text{-}LIBS}$-DOTA. The utility of $scFv_{anti\text{-}LIBS}$-MeCOSar as a diagnostic agent was assessed *in vivo* in a mouse model of acute thrombosis. The uptake of $scFv_{anti\text{-}LIBS}$-^{64}CuMeCOSar in the injured vessel was significantly higher than the non-injured vessel. Positron-emission tomography was used to show accumulation of $scFv_{anti\text{-}LIBS}$-^{64}CuMeCOSar with high and specific uptake in the injured vessel. $ScFv_{anti\text{-}LIBS}$-^{64}CuMeCOSar is an excellent tool for highly sensitive *in vivo* detection of activated platelets in PET and has the potential to be used for early diagnosis of acute thrombotic events.

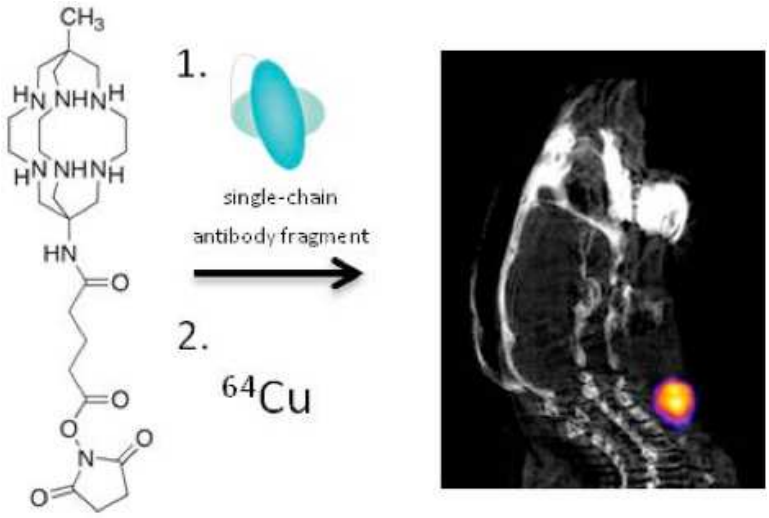

Key words: Platelets, Integrin GPIIb/IIIa, Single-chain antibody, Positron emission tomography, ^{64}Cu chelator

INTRODUCTION

Acute thrombotic events such as myocardial infarction or ischemic stroke, leading causes of mortality, morbidity and long-term disability, are often associated with the rupture of atherosclerotic plaques.[1] The atherosclerotic plaque is often indolent and typically destabilises without warning, resulting in plaque rupture and intravascular thrombosis. Over the last decade it has been recognised that activated platelets are not only a key part of thrombosis but also integral to inflammatory diseases including atherosclerosis.[2-4]

Current practice to diagnose coronary artery disease is angiography of patients who present with symptoms of angina but a limitation of this regimen is that it does not detect unstable vulnerable plaques that are prone to rupture. Molecular imaging with positron emission tomography (PET) has the potential to detect small numbers of platelets as hallmarks of inflamed rupture prone plaques.

Radioimmunoconjugates, antibodies attached to a radiolabelled bifunctional chelator (BFC), combine the selectively of antibodies for activated platelets with the imaging possibilities of PET and could be valuable tools to assist in the diagnosis of acute thrombosis or inflammation. A single-chain variable fragment $scFv_{anti\text{-}LIBS}$, which targets the ligand-induced binding sites (LIBS) on the glycoprotein receptor GPIIb/IIIa of human and mouse platelets has considerable potential as a diagnostic tool.[5-7] The high abundance of activated GPIIb/IIIa receptors on activated platelets and the fact that the $scFv_{anti\text{-}LIBS}$ does not compromise function and has no effect on platelets aggregation makes this antibody ideal for molecular imaging of thrombosis and inflammation.[8,9]

Copper-64 (^{64}Cu), a positron emitter with a half-life of 12.7 hours and a positron emission energy of 0.657 MeV which is almost identical to ^{18}F (0.635 MeV), is an attractive radioisotope for molecular imaging of antibody fragments.[10-14] Several BFCs have been reported for complexing $^{64}Cu^{II}$ but acceptable radiochemical yields often require heating to temperatures not compatible with biologics.[14,15] The hexaaminemacrobicyclic cage ligands or sarcophagines (sar) form complexes with Cu^{II} that are remarkably thermodynamically stable and kinetically inert and coordinate $^{64}Cu^{II}$ with fast complexation kinetics at room temperature even at low concentrations. These unique features make these ligands particularly well suited for copper radioimmunoconjugates.[16-20]

Herein, we present the synthesis and characterisation of a *N*-hydroxysuccinimide (NHS) ester of a methyl capped sar derivative, 2,5-dioxopyrrolidin-1-yl 5-(8-methyl-3,6,10,13,16,19-hexaaza-bicyclo[6.6.6]icosan-1-ylamino)-5-oxopentanoate (MeCOSar-NHS-ester) (Figure 1A) and use it and 2,2′,2″-(10-(2-((2,5-dioxopyrrolidin-1-yl)oxy)-2-oxoethyl)-

1,4,7,10-tetraazacyclododecane-1,4,7-triyl)triacetic acid (DOTA-NHS-ester) (Figure 1B) to form conjugates with $scFv_{anti\text{-}LIBS}$. After conjugation to $scFv_{anti\text{-}LIBS}$, the optimal conditions for radiolabelling the BFC-$scFv_{anti\text{-}LIBS}$ conjugates were determined and biological activity was assessed using flow cytometry. Selective uptake of $scFv_{anti\text{-}LIBS}$-^{64}CuMeCOSar in a carotid artery mouse model was demonstrated by PET.

RESULTS

Synthesis of MeCOSar-NHS-ester, conjugation to $scFv_{anti\text{-}LIBS}$ and radiolabelling with $^{64}Cu^{II}$.

The activated ester, (t-Boc)$_{4\text{-}5}$MeCOSar-NHS-ester, was obtained by reacting (t-Boc)$_{4\text{-}5}$MeCOSar with 1-ethyl-3-(3-dimethylaminopropyl)carbodiimide (EDC) and N-hydroxysuccinimide (NHS) in DMF, followed by purification by silica gel chromatography. The t-Boc groups were removed with trifluoroacetic acid and MeCOSar-NHS-ester was isolated as the tris-trifluoroacetic acid tris-hydrate salt (Figure 1A). The NMR spectra of MeCOSar-NHS-ester in d_6-dmso indicated complete removal of the t-Boc groups and a single NHS activated ester group (Figure 1B).

The scFv constructs were incubated with various molar equivalents of both DOTA-NHS-ester, in 0.1 M Na_2HPO_4 for 24 hours at 4 °C, and MeCOSar-NHS-ester, in borate buffer (pH 8.4) for 3 hours at room temperature.[21-23] The binding of each immunoconjugate to activated platelets was investigated using flow cytometry. Activated and non-activated platelets were incubated with 2 μg/mL of each tracer and stained with anti penta-Alexa-Fluor-488 antibody. The antibody binding fell to 7%, 20% and 86% when compared to non modified $scFv_{anti\text{-}LIBS}$ when using 5×, 15× and 30× excess (molar ratios) of MeCOSar-NHS-ester, respectively. In comparison, the DOTA-NHS-ester results indicated a binding reduction of 11%, 50% and 65% with 5×, 15× and 30× molar excess, respectively (Figure 1C). After radiolabelling with $^{64}Cu^{II}$ the amount of radioactivity associated with each immunoconjugate was determined by thin-layer-chromatography. An increase in the molar ratio of chelator to $scFv_{anti\text{-}LIBS}$ resulted in an increase in specific activity for both constructs. The flow cytometry showed $scFv_{anti\text{-}LIBS}$ target binding decreased as the molar equivalents of bifunctional chelator used in the conjugation increased but the use of higher molar equivalents of chelator increased the specific activity (Figure 1C). A 15× molar excess led to the best compromise between the specific activity of the radioimmunoconjugate and reduction in antibody efficacy (only 15-20% reduction in antibody binding as assessed by flow cytometry). From ESI-TOF MS data (not shown) we can estimate up to 5 MeCOSar or DOTA per scFv with an average

loading of 2-3 MeCOSar or DOTA after modification with a15× molar excess. Importantly, the binding of radiolabelled $scFv_{anti\text{-}LIBS}$-^{64}CuMeCOSar to activated platelets was comparable to that of $scFv_{anti\text{-}LIBS}$-MeCOSar (Figure 2A). As expected, neither construct bound to non-activated platelets (Figure 2B). A mutated version of the $scFv_{anti\text{-}LIBS}$ ($scFv_{mut}$) showed no binding to activated (Figure 2C) and non-activated platelets (Figure 2D) and served to highlight the specificity of $scFv_{anti\text{-}LIBS}$-MeCOSar.

PET imaging

Both $scFv_{anti\text{-}LIBS}$-^{64}CuMeCOSar and $scFv_{mut}$-^{64}CuMeCOSar immunoconjugates were tested in an *in vivo* model of mouse carotid artery thrombosis using BALB/c mice. The tracers were injected intravenously, the mice were placed in a small animal PET/CT scanner and the carotid artery was set as the region of interest to achieve the highest sensitivity in the center of the PET detector ring. PET image acquisition began 5 minutes post-injection, directly followed by a CT scan without moving the animal (Figure 3). The standardized uptake values (SUV) for $scFv_{anti\text{-}LIBS}$-^{64}CuMeCOSar showed specific and strong accumulation of the tracer in the injured vessel (3.5 ± 0.34) compared to the control vessel (0.25 ± 0.17) and soft tissue (0.15 ± 0.094, p = 0.0001, n = 6) 90 minutes after tracer injection (total time for PET and CT). In contrast, the mutant control immunoconjugate, $scFv_{mut}$-^{64}CuMeCOSar, showed only minor tracer uptake in the injured vessel with no significant difference between injured (0.92 ± 0.67) and non-injured vessels (0.19 ± 0.16, ns, n = 6) 90 minutes after tracer injection. The injured vessel/soft tissue SUV ratio was significantly higher compared to the intact vessel/soft tissue SUV ratio 60 minutes after tracer injection (Table 1). We also tested $scFv_{anti\text{-}LIBS}$-^{64}CuDOTA and $scFv_{mut}$-^{64}CuDOTA in this animal model but could not obtain significant results (data not shown) because of the low specific activity (see Fig 1C) of these constructs.

Blood immunoreactivity, biodistribution and immunohistology

Over 90% of the tracer was cleared from the blood approximately 30 minutes after injection (Figure 4). The full biodistribution data show that $scFv_{anti\text{-}LIBS}$-^{64}CuMeCOSar was excreted rapidly *via* the renal pathway as demonstrated by the high activity in the kidney and bladder relative to other organs (Table 2). In agreement with the data from the PET imaging a significant increase in $scFv_{anti\text{-}LIBS}$-^{64}CuMeCOSar uptake in the injured vessel (108.5 ± 47.5 %ID/g) compared to non-injured vessel (12.8 ± 5.2 %ID/g, p = 0.001, n = 6) was observed. There was also significantly higher uptake of $scFv_{anti\text{-}LIBS}$-^{64}CuMeCOSar in the injured vessel

compared to $scFv_{mut}$-^{64}CuMeCOSar (8.5 ± 8.4 %ID/g, p = 0.001, n = 6). $ScFv_{mut}$-^{64}CuMeCOSar uptake in the injured vessel, control vessel and in the muscle revealed only a minimal background signal, 90 minutes after injection (Figure 5A). In a separate study, administration of $scFv_{anti\text{-}LIBS}$ (400 µg) 30 minutes before radiotracer injection significantly reduced $scFv_{anti\text{-}LIBS}$-^{64}CuMeCOSar binding to the target receptor (p = 0.001, n = 5) (Figure 5B).

Immunohistology on the resected carotid vessels confirmed the presence of platelets with the platelet marker CD41 in vessels that were exposed to $FeCl_3$ solution (Figure 6A) but not in non-injured vessels (Figure 6C). PBS was used as a control (Figure 6B). In all animals assessed with this method, the injured vessel developed a thrombus within 20 minutes of exposure to $FeCl_3$ solution.

DISCUSSION

Platelets are the main mediators of haemostasis and are also integral to important inflammatory processes. Novel imaging agents with high sensitivity and specificity for activated platelets have the potential to detect acute thrombotic events in severe disease such as stroke and myocardial infarction as well as to detect platelets in inflammatory disease such as arthritis and atherosclerosis.[24] Several bifunctional chelators have been reported that enable the incorporation of radioactive metal ions into antibodies but their conjugation to the antibody can have a negative impact on biological function and half-life.[25]

In this manuscript we describe the synthesis and isolation of a cage amine (sarcophagine) chelator as a NHS-activated ester for bioconjugation reactions with proteins and antibodies. The sarcophagine family of cage amine ligands are well suited for applications involving radioactive copper isotopes as these ligands form extremely stable complexes with Cu^{II} with fast complexation kinetics at room temperature even at low concentrations.[16-20]

Attachment of bifunctional chelators to antibodies is often achieved by generating an activated ester *in situ* from carboxylate functional groups on either the chelator or the antibody by using an excess of both ligand and coupling reagents such as 1-ethyl-3-(3-dimethylaminopropyl)carbodiimide (EDC).[21,26] When activated esters are generated *in situ* it is often necessary to use a large excess of the BFC and coupling agent to achieve reasonable incorporation, and reduce competing side-reactions.

The reaction of MeCOSar with a stoichiometric excess of di-*tert*-butyl dicarbonate resulted in a mixture of products and regioisomers where either four or five of the six

available secondary amines have reacted to form *N*-*tert*-butoxycarbonyl functional groups.[27] This protection of the secondary amines prevents their reaction with the activated ester as it is formed in the following step and has the added benefit of improving the solubility in the organic solvents used to prepare and purify the activated NHS-ester. The reaction of (*t*-Boc)$_{4\text{-}5}$MeCOSar with EDC and *N*-hydroxysuccinimide (NHS) in DMF, followed by purification by silica gel chromatography allows isolation of the activated ester, (*t*-Boc)$_{4\text{-}5}$MeCOSar-NHS-ester in good yield. Deprotection with trifluoroacetic acid leads to the isolation of MeCOSar-NHS-ester as the tris-trifluoroacetic acid tris-hydrate salt. The NMR spectra of MeCOSar-NHS-ester in d_6-dmso is as expected and the compound is stable when dissolved in DMSO for at least several weeks. The tris-trifluoroacetic acid tris-hydrate salt is stable (with respect to hydrolysis of the NHS-ester) for several months when stored anhydrous and at low temperatures. This stability means that this activated ester of sarcophagine is a versatile and reliable reagent for the modification of proteins, antibodies and peptides and is ideally suited for widespread application of the sarcophagine family of ligands to nuclear medicine applications.

ScFv$_{anti\text{-}LIBS}$-^{64}CuMeCOSar was labelled with ^{64}Cu under milder conditions (pH 8, 30 minutes, room temperature) when compared to the formation of scFv$_{anti\text{-}LIBS}$-^{64}CuDOTA (pH 5, 45 minutes, 40 °C).[21,22] As expected, the use of increasing molar excesses of both chelators to scFv in the conjugation reaction resulted in products with more ligands attached to the scFv$_{anti\text{-}LIBS}$ but also compromised the biological activity of the antibody. Clear differences in the specific activity between the immunoconjugates were observed. ScFv$_{anti\text{-}LIBS}$-^{64}CuMeCOSar produced using 15× molar excess of MeCOSar was judged to be the optimal conjugation product due to the best compromise between high specific activity and target receptor binding.

The scFv$_{anti\text{-}LIBS}$-^{64}CuMeCOSar radioimmunoconjugate showed typical fast blood clearance and renal excretion.[28-30] Fast clearance is ideal for imaging acute thrombosis where the time frame for obtaining images is relatively narrow[31]. The high uptake of scFv$_{anti\text{-}LIBS}$-^{64}CuMeCOSar in the kidney and bladder relative to other organs is comparable to radiolabelled peptides featuring an Arg-Gly-Asp (RGD) sequence that are used as radiotracers to detect integrin expression.[32] Imaging $\alpha_v\beta_3$ integrin with RGD peptides as a marker of angiogenesis has proved valuable to the clinical diagnosis and treatment of certain cancers. The $\alpha_v\beta_3$ integrin receptor is also expressed by macrophages in atherosclerotic lesions and selected RGD peptides are cross-reactive to the GPIIb/IIIa integrin for the detection of platelets.[33] However, in contrast to the scFv$_{anti\text{-}LIBS}$, RGD peptides are integrin

agonists causing platelet activation and are therefore not optimal for diagnostic imaging in patients.[34,35]

There was relatively low levels of radioactivity measured in the liver, in contrast to copper radiopharmaceuticals using other chelating agents.[26] It has been reported that Cu-DOTA conjugates are not sufficiently stable *in vivo* with ^{64}Cu exchanging with proteins such as superoxide dismutase, which ultimately results in an accumulation of ^{64}Cu in the liver.[36,37]

This premature ^{64}Cu release *in vivo* could in part explain the lack of PET signal in the target tissue after the injection of $scFv_{anti\text{-}LIBS}$-^{64}CuDOTA. Furthermore, DOTA requires much higher temperatures (85-95C) for optimal loading which is incompatible with biological molecules. In addition, DOTA handling and labelling requires a metal free environment and additional cleaning steps of equipment and solutions. Our study was carried out under normal laboratory conditions with reasonable precautions to keep metal contaminations low. Our results demonstrate the superior and most specific Cu complexation of MeCOSar compared to DOTA. By using the next generation MeCOSar for PET imaging, the additional precautions and treatment steps for DOTA labelling are not required thereby broadening the potential use of ^{64}Cu in PET.

The $FeCl_3$ induced vascular thrombosis is a very common model of vascular injury. Full vessel occlusion can be achieved with 10% $FeCl_3$ or greater. Lower concentration of $FeCl_3$, as used in this study, results in non-occlusive stenosis mimicking the development of human lesions, where activated platelets build up on the surface of a plaque.

In summary, we have reported the synthesis and isolation of an activated ester of a sarcophagine cage amine chelator and demonstrated that it is a versatile and reliable reagent for the modification of a scFv against the platelet integrin GPIIb/IIIa in its active, ligand bound form. The new immunoconjugate was radiolabelled with $^{64}Cu^{II}$ under mild conditions with high specific activity to give $scFv_{anti\text{-}LIBS}$-^{64}CuMeCOSar.

EXPERIMENTAL SECTION

General

DOTA-NHS-ester (Product no. B-280) was purchased from Macrocyclics, TX, USA. All other reagents and solvents were obtained from standard commercial sources and were used as received. The compound (*t*-Boc)$_{4\text{-}5}$MeCOSar was synthesized as previously described.[27] Nuclear magnetic resonance (NMR) spectra were acquired on Varian FT-NMR 500 and 400 spectrometers. Chemical shifts were referenced to the residual solvent peak. ESIMS spectra

were recorded on an Agilent 6510 esi-TOF LC/MS mass spectrometer (Agilent, Palo Alto, CA).

Synthesis of (*t*-Boc)$_{4\text{-}5}$MeCOSar-NHS-ester

To a solution of (*t*-Boc)$_{4\text{-}5}$MeCOSar (0.05 g, 0.055 mmol), consisting of a mixture of *N*-*tert*-butoxycarbonyl (*t*-Boc) regioisomers, in dry DMF (1 mL) was added 1-ethyl-3-(3-dimethylaminopropyl)carbodiimide (0.02 g, 0.11 mmoL) followed by *N*-hydroxysuccinimide (0.01 g, 0.11 mmoL). The clear solution was stirred under a nitrogen atmosphere at 60 ºC for 3.5 hours. The reaction was monitored by ESI-MS. The solvent was removed *in vacuo* and the residue was extracted with dichloromethane (100 mL) and washed with water (100 mL ×3). The organic phase was dried over anhydrous $MgSO_4$, filtered and evaporated to dryness and purified by flash chromatography on silica gel (mobile phase: dichloromethane/methanol = 100/2 (v/v)) to give a mixture of *t*-Boc regioisomers as a white solid (0.023 g, 46% approx. yield based on four *t*-Boc groups). ^{1}H NMR (400 MHz, $CDCl_3$, 25 ºC): δ = 1.47, s, $(CH_3)_3$; 2.81, s, 4H, CH_2 (NHS). ^{13}C NMR (100 MHz, $CDCl_3$, 25 °C): δ = 20.6. CH_3; 25.7, CH_2; 28.6, $(CH_3)_3$, CH_2; 30.4, CH_2. Further NMR assignments proved problematic due to the mixture of regioisomers. ESI-MS: (+ve ion) [$C_{44}H_{77}N_8O_{13}$ + H^+] m/z 100% 925.56 (experimental), 925.56 (calcd), [$C_{49}H_{85}N_8O_{15}$ + H^+] m/z 100% 1025.61 (experimental), 1025.61 (calcd).

Synthesis of MeCOSar-NHS-ester

To a solution of (*t*-Boc)$_{4\text{-}5}$MeCOSar-NHS-ester (0.023 g, 0.025 mmol) in dichloromethane (5 mL) was added trifluoroacetic acid (5 mL). The mixture was shaken at room temperature for 3 h. The solution was sparged with N_2 to reduce the volume to 1 mL. Cold diethyl ether (45 mL) was added to precipitate a white solid. Following centrifugation (3 minutes, 4000 rpm) the ether layer was removed by decanting and the procedure was repeated. Finally, the majority of the residual diethyl ether was removed *in vacuo* and the tris-trifluoroacetic acid tris-hydrate salt of the title compound was isolated. (0.017 g, 71% approx. yield based on four *t*-Boc groups). (Found: C, 39.58; H, 5.65; N, 11.84; calcd for $C_{24}H_{44}N_8O_5 \cdot 3(C_2HF_3O_2) \cdot 3(H_2O) \cdot 0.2(C_4H_{10}O)$: C, 39.54; H, 5.93; N, 11.98). ^{1}H NMR (500 MHz, d_6-dmso, 25 °C): δ = 0.86, s, 3H, CH_3; 1.09, t, CH_3 (Et_2O); 1.84, m, 2H, CH_2; 2.27, t, ^{3}J = 7.5 Hz, 2H, CH_2; 2.72, t, ^{3}J = 7.5 Hz, 2H, CH_2; 2.82, s, 4H, CH_2 (NHS); 2.9-3.2, br m, 24H, cage CH_2. ^{13}C NMR (125.7 MHz, d_6-dmso, 25 °C): δ = 15.2, CH_3 (Et_2O); 19.7, CH_3; 20.0, CH_2; 25.4, CH_2 (NHS); 29.5, 34.0, CH_2; 36.7, quat. C of methyl cage cap; 45.8, 47.2,

50.6, 53.2, cage CH_2; 56.5, quat. C of amine cage cap; 64.9, CH_2 (Et_2O); 117.0, q, $^1J_{CF}$ = 299 Hz, CF_3; 158.3, q, $^2J_{CF}$ = 31 Hz, *C*OCF_3; 168.8, CO; 170.2, CO (NHS); 173.6, CO. ESI-MS: (+ve ion) [$C_{24}H_{44}N_8O_5 + H^+$] m/z 100% 525.35 (experimental), 525.35 (calcd).

Production of the scFv

Production, characterisation and purification of scFv have been described previously.[8,38] Briefly, the scFv was produced in TG1 *E. coli* transformed with a pHOG expression vector containing the sequence for the scFv with a histidine protein purification tag. Bacterial pellets were collected from 1 litre cultures that were allowed to grow for 5 hours at 37 °C. A lysate was produced using a protein extraction buffer according to the manufacturers instruction (BugBuster, Merck/Novagen). The lysate was cleared and his-tagged antibodies were extracted from the cleared lysate on a FPLC system with 5 mL columns packed with Ni-agarose beads (Ni-NTA Superflow cartridge, Qiagen). The captured scFv was eluted from the column with 250 mM imidazole, fractions containing high levels of protein were dialysed against PBS (pH 7.2) to remove excess imidazole. The antibody was further polished by size exclusion chromatography. Samples of fractions from the purification were analysed by SDS-PAGE under reducing conditions. Final purity was over 95% according to SDS page analysis. The binding of the purified antibody was evaluated using flow cytometry. Final concentration of purified antibody was determined using BCA protein assay (Pierce, Thermo Scientific).

Flow cytometry

Flow cytometry was done as described previously.[8,38] Briefly, fresh citrated blood from healthy volunteers was centrifuged at 180*g* for 10 minutes to obtain platelet rich plasma (PRP). Non-activated and activated platelets (stimulated with 20 μM adenosine diphosphate, ADP, Sigma) were incubated with scFv at room temperature. After 15 min platelets were incubated for another 10 min in the dark at room temperature with the Penta His Alexa-488 secondary antibody (1:1000)(Qiagen) which selectively binds to the histidine-tag. Then platelets were fixed and relative fluorescence of stained cells was measured on a BD FACScalibur flow cytometer. Fluorescence signal was examined on 10,000 gated events and analysed using the CellQuest software (Becton Dickenson).

Preparation of $scFv_{anti\text{-}LIBS}$-DOTA

The $scFv_{anti\text{-}LIBS}$ (5 mg/mL) was dialysed against 0.1 M Na_2HPO_4 (pH 7.5) containing 1.2 g/L Chelex 100 (Fluka) overnight at 4 °C. Three different reactions were prepared with either 70.6 µL, 17.52 µL or 5.84 µL of freshly prepared 30 mg/mL DOTA-NHS-ester in 0.1 M Na_2HPO_4 added to the scFv. The reaction mixtures were incubated at 4 °C for 24 h under continuous shaking, and dialysed against 10 mM Na_2HPO_4, 150 mM NaCl (pH 7.5) and 1.2 g/L Chelex 100. The conjugates were dialysed against 0.25 M ammonium acetate (pH 7.0) containing 1.2 g/L Chelex 100 and transferred to a 1.5 mL reaction tube.

Preparation of $scFv_{anti\text{-}LIBS}$-MeCOSar

The $scFv_{anti\text{-}LIBS}$ was buffer exchanged and concentrated to 5 mg/mL in borate buffer (50 mL of 0.2 M solution of boric acid, 22.5 mL of solution of borax, diluted to a total volume of 200 mL, pH 8.7) in centrifugation tubes and transferred to a 1.5 mL plastic tube. Three different reactions were prepared with either 93 µL, 23.24 µL or 7.75 µL freshly prepared 16 mg/mL MeCOSar-NHS-ester in DMSO added to the scFv. The reaction mixtures were incubated at room temperature for 3 h with continuous end-over-end mixing, dialysed against borate buffer in centrifugation tubes and transferred to a 1.5 mL plastic tube.

^{64}Cu-production

No-carrier-added ^{64}Cu was produced with the IBA Nirta target by the ^{64}Ni(p,n)^{64}Cu reaction. The target was produced by direct electroplating of highly enriched ^{64}Ni (> 99%, Isoflex USA) onto an Ag disk (24 mm diam x 1.0 mm thick disk). The plating cell was filled with ^{64}Ni solution + NH_4OH (total = 55 mL) and electroplating was carried out at 5.0 mA using a chopped saw tooth current for ~12-24 hrs to give an average 20-50 µm ^{64}Ni thickness.

Targets were irradiated using an IBA 18/9 cyclotron with an incident beam of 14.9 Mev (18 MeV degraded by 0.5 mm aluminium foil). The irradiated disk was then loaded into an IBA Pinctada module and the ^{64}Ni plating dissolved in recirculating 3 mL 9-12 M HCl at 70°C using a peristaltic pump. Once dissolved, the solution was loaded onto an AG 1-X8 anion exchange cartridge for purification and the cartridge is washed with various concentrations of HCl to recover the ^{64}Ni and elute impurities such as ^{61}Co. ^{64}Cu was recovered in ~2 mL of water. Typical production yields average 30 mCi EOS for a 4 hr irradiation at 35 µA with a ^{64}Ni thickness of 25 µm (EOS 12 hrs post EOB).[39]

Radiolabelling

DOTA radiolabelling was performed according to a modified procedure.[20] Briefly, $scFv_{anti\text{-}LIBS}$-DOTA (100 µg) in 1.5-mL reaction tubes (0.25 M NH_4OAc, pH 7.0) was incubated with approximately 25-35 MBq of ^{64}Cu in 0.01 M HCl at 40 °C for 40 min with continuous shaking (final pH 5.5). A solution of 10 mM diethylenetriaminepentaacetic acid (10 µL) was added and the reaction incubated for 5 min. $ScFv_{anti\text{-}LIBS}$-MeCOSar (100 µg) was incubated with 25-35 MBq of ^{64}Cu in borate buffer at room temperature for 30 min. A solution of 10 mM ethylenediaminetetraacetic acid (10 µL) was added and the reaction incubated for 5 min. All samples were washed twice with PBS using spin columns (Millipore, cut off 10,000 MWCO). Analysis/Quality control was performed using thin layer chromatography (silica gel 60, F254; Merck) and 0.1 M citrate buffer (pH 5) as the mobile phase. Radiolabelled immunoconjugate (1.5 µL) was spotted at the origin, the strip was allowed to air-dry and was developed. The strip was cut into three pieces and the radioactivity in each section was counted using a gamma counter (Wizard single-detector gamma-counter, Perkin Elmer).

Blood clearance

For the determination of blood clearance in healthy BALB/c mice, $scFv_{anti\text{-}LIBS}$-MeCOSar labelled with ^{64}Cu was injected *via* a lateral tail vein into three animals at a single dose of 20 µg. Blood was collected at different time points between 15 minutes and 24 hours after tracer injection. Then, the samples were measured in a gamma counter (Wizard single-detector gamma-counter, Perkin Elmer) using an energy window between 425 and 640 keV. Results are expressed as percentage injected dose (%ID) per gram of blood.

PET studies and post-mortem biodistribution

Thrombosis was induced as described.[8,38] Six-week-old BALB/c (21-23g) were anesthetised with ketamine (50 mg/kg; Parnell Laboratories) and xylazine (10 mg/kg; Troy Laboratories) and placed on a 37 °C heater mat to prevent hypothermia. The left common carotid artery was dissected from circumferential connective tissues. A small piece of plastic was placed under the vessel to protect surrounding tissue and was followed by placing a small filter paper saturated with 6% ferric chloride under the carotid artery of the animal for 3 minutes to induce formation of a non-occlusive thrombus. The animals were injected via a lateral tail vein 20 min after injury with $scFv_{anti\text{-}LIBS}$-^{64}CuMeCOSar or the control (20 µg, 3-5 MBq). A 1 h PET scan was acquired starting 5 min after tracer injection using a NanoPET/CT preclinical imager (Bioscan, Washington DC, USA) with a 60 min PET acquisition time, and

coincidence relation of 1-3. Image reconstruction of the entire 60 min data set was performed with the following parameters- OSEM with SSRB 2D LOR, energy window, 400-600 keV; filter Ramlak cut off 1, number of iteration/subsets, 8/6. For the CT scans, an X-ray voltage of 45 kVp, an exposure time of 900 ms and a pitch of 0.5 were used. A total projection of 240 projects over 360° of rotation was acquired. Projection data were rebinned by 1:4 and reconstructed using a RamLak filter, into a matrix having an isotropic voxel size of 96 μm. During imaging, the animals were anesthetized with a mixture of 1.5% isoflurane and 100% oxygen. The animal bed was heated. Image files of PET and CT scan were fused and analysed using the analysis software InVivoScope version 2.00. The radioactivity concentrations in the PET images were recalculated to provide images of Standardized Uptake Value (SUV) by dividing the radioactivity concentration (Bq/mL) by the injected radioactivity (Bq) per body weight (g).

After the CT scan the animals were perfused with PBS, the injured and control vessel as well muscle were removed, wet-weight measured on a high precision balance and the level of radioactivity determined with an aliquot of injected solution as standard in the gamma counter (Perkin Elmer) using an energy window between 450 and 650 keV. Results were expressed as % injected dose per g (% ID/g) of tissue. All experiments involving animals were approved by the Alfred Medical Research and Education Precinct Animal Ethics Committee (E/1232/2012/B).

Histochemistry

Histochemistry was conducted as reported previously.[7] The injured carotid arteries were removed, embedded in OCT TissueTec (Sakura Fine technical, Japan). Tissue was cut in transverse sections of 10 μm at intervals of 30 μm. Tissue sections of 6 μm were prepared from formalin fixed carotid artery. The sections were treated with 3% hydrogen peroxide in methanol prior to antigen retrieval with 20μg/mL of Proteinase K buffer solution. To reduce non-specific staining, tissue section were blocked with normal serum, avidin and biotin (Vector Laboratories, CA) solutions. Rat anti-mouse CD41 IgG antibody (AbD Serotec, clone: MWReg30) at 5μg/mL or PBS were added for overnight incubation at 4^{o}C. Subsequent steps were performed using Vectastain ABC kit (Vector Laboratories) in which sections were incubated with biotinylated anti-rat IgG antibody followed by ABC reagent. The staining was developed using 3,3'-Diaminobenzidine **(**DAB**)-**peroxidase substrate for 5 minutes. The sections were counterstained with Mayer's Hematoxylin and slides mounted.

The section was examined under the microscope for brown DAB stains which indicated presence of CD41.

Statistical analysis

All quantitative data is reported as mean +/- standard deviation. Statistical analysis was performed using ANOVA followed by Tukey's multiple comparison test; data was considered as statistically significant for *p* values of 0.05 or less.

FIGURES

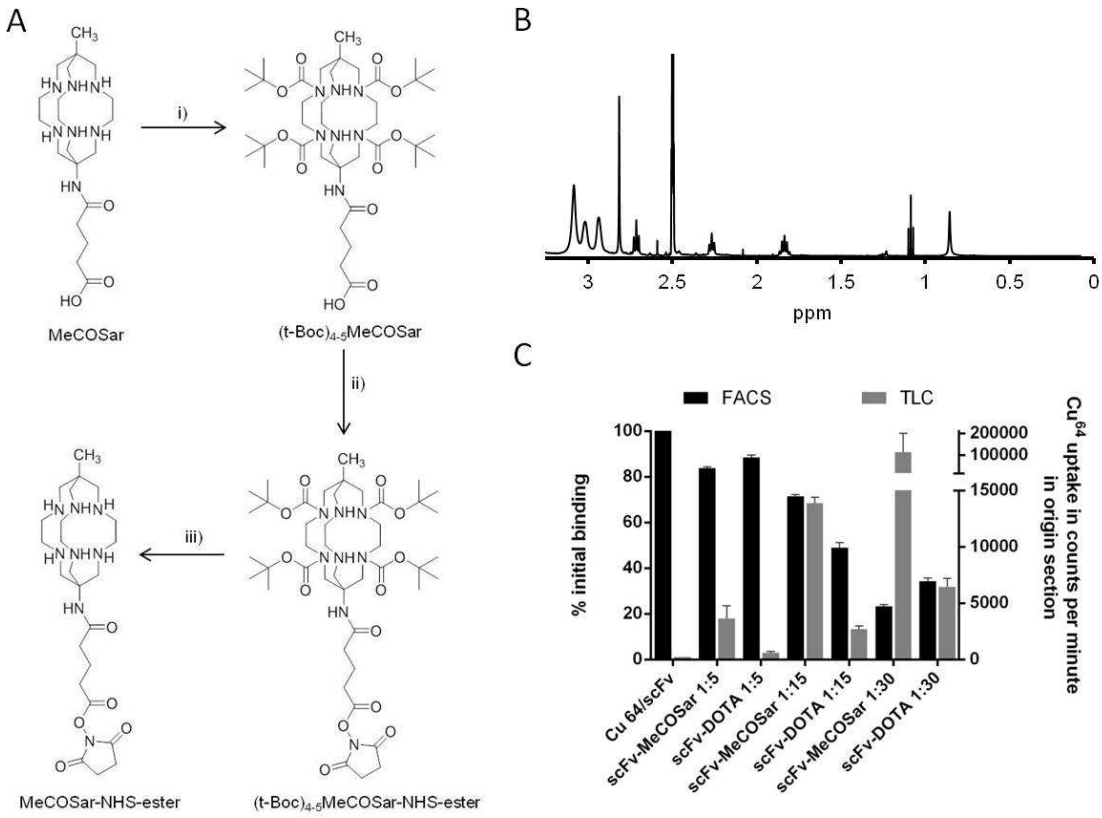

Figure 1: A) Synthesis of MeCOSar-NHS-ester. (i) Boc_2O, Et_3N, H_2O/THF; (ii) 1-ethyl-3-(3-dimethylaminopropyl)carbodiimide, *N*-hydroxysuccinimide, DMF; (iii) trifluoroacetic acid, CH_2Cl_2, Et_2O. B) ^1H NMR spectrum of MeCOSar-NHS-ester in d_6-dmso. C) Antibody binding compared to ^{64}Cu radiochemical purity for $scFv_{anti\text{-}LIBS}$-MeCOSar and $scFv_{anti\text{-}LIBS}$-DOTA. An increasing number of ^{64}Cu chelators attached to the $scFv_{anti\text{-}LIBS}$ as measured by thin layer chromatography led to higher specific activity (grey bar) as well as decreased $scFv_{anti\text{-}LIBS}$ binding as measured by flow cytometry (black bar), n=3.

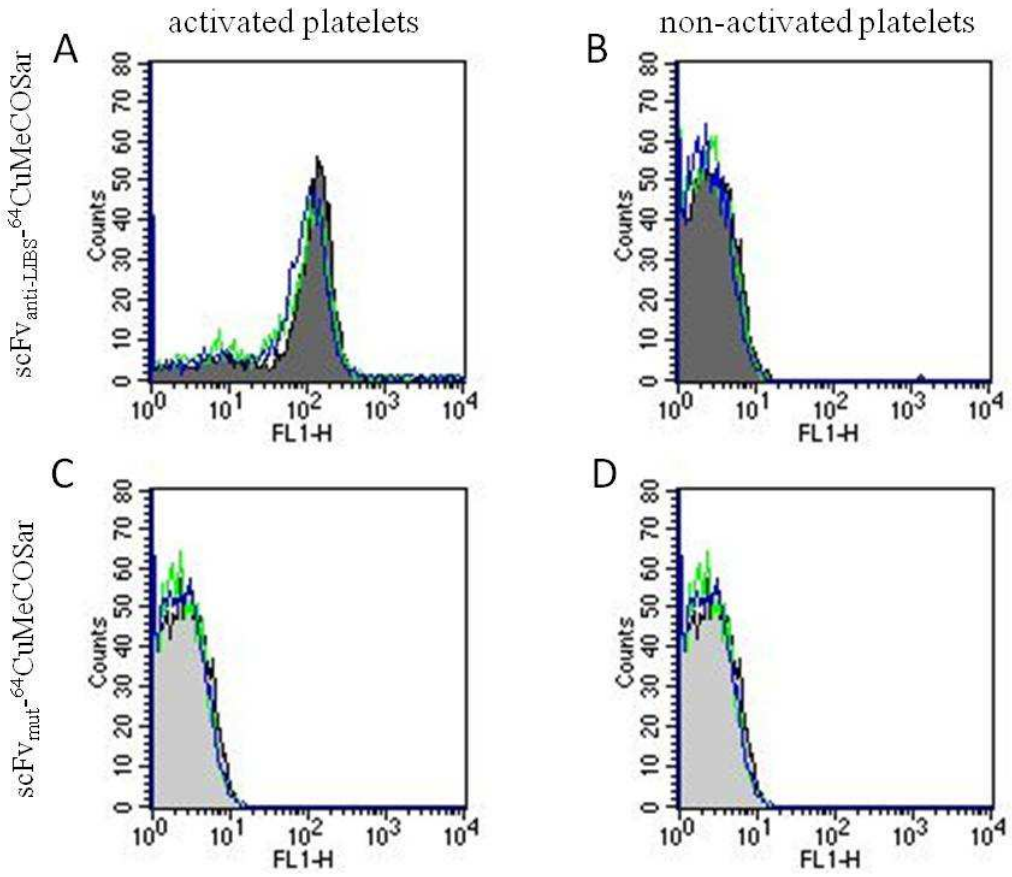

Figure 2: Binding of conformation-specific scFv$_{anti-LIBS}$ and scFv$_{mut}$ to activated and non-activated human platelets. Histogram shows binding of ADP-stimulated platelets of initial scFv$_{anti-LIBS}$ (grey highlighted) compared to modified scFv$_{anti-LIBS}$-MeCOSar (green line) and radiolabelled scFv$_{anti-LIBS}$-^{64}CuMeCOSar (blue line) (A) and non-activated platelets (B) in flow cytometry. Graphic indicates preserved binding of the scFv$_{anti-LIBS}$ constructs. ScFv$_{mut}$ constructs indicated no binding to activated (C) or non-activated platelets (D). Representative histograms out of n=3 is shown.

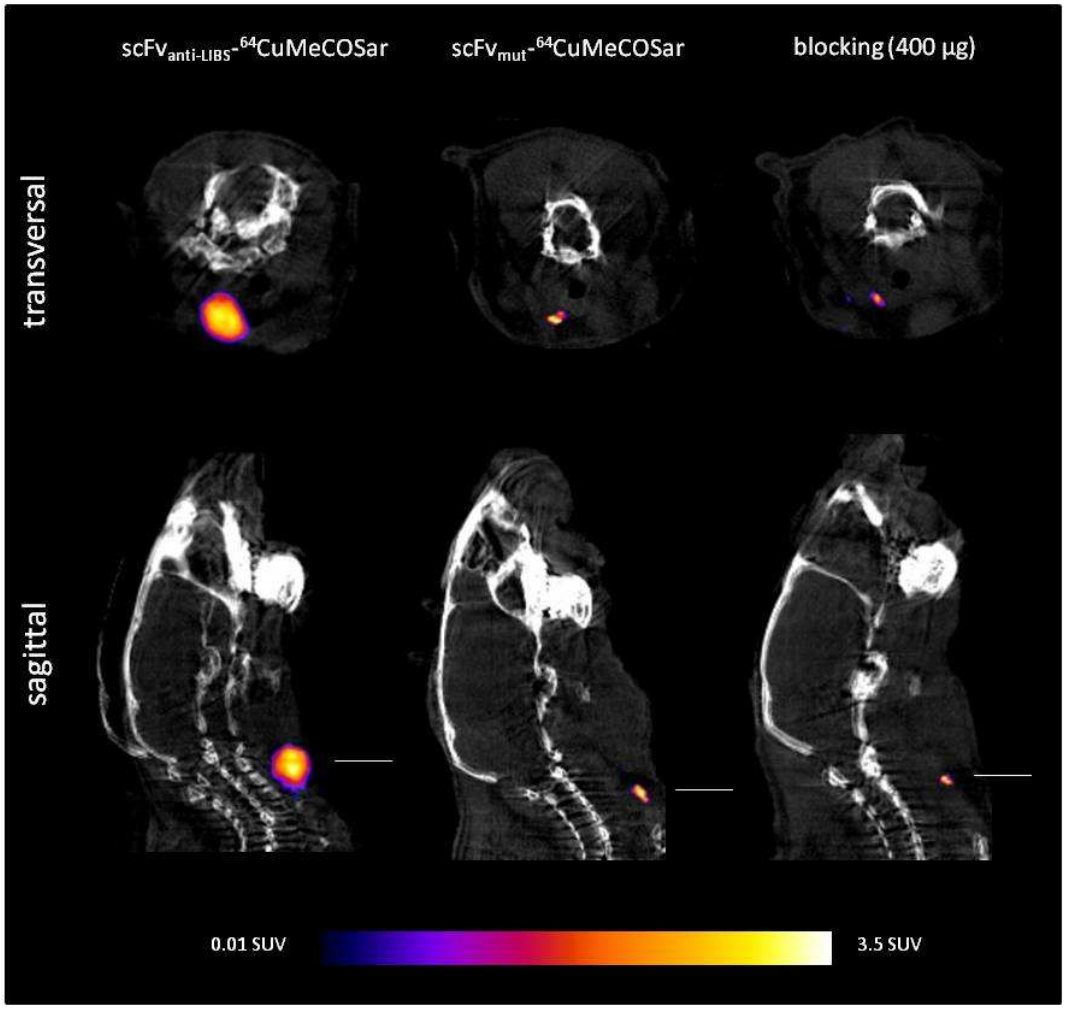

Figure 3: Serial small-animal PET images of an *in vivo* model of mouse carotid artery thrombosis 60 min after injection of the radiotracer. Comparison of representative transverse and sagittal PET images of scFv$_{anti-LIBS}$-^{64}CuMeCOSar, scFv$_{mut}$-^{64}CuMeCOSar and a blocking experiment by injecting scFv$_{anti-LIBS}$ 30 min before injection of scFv$_{anti-LIBS}$-^{64}CuMeCOSar is shown (n = 6). The colour scale for all PET image data shows radiotracer uptake in units of standard uptake value (SUV), with white corresponding to the highest activity and blue to the lowest activity.

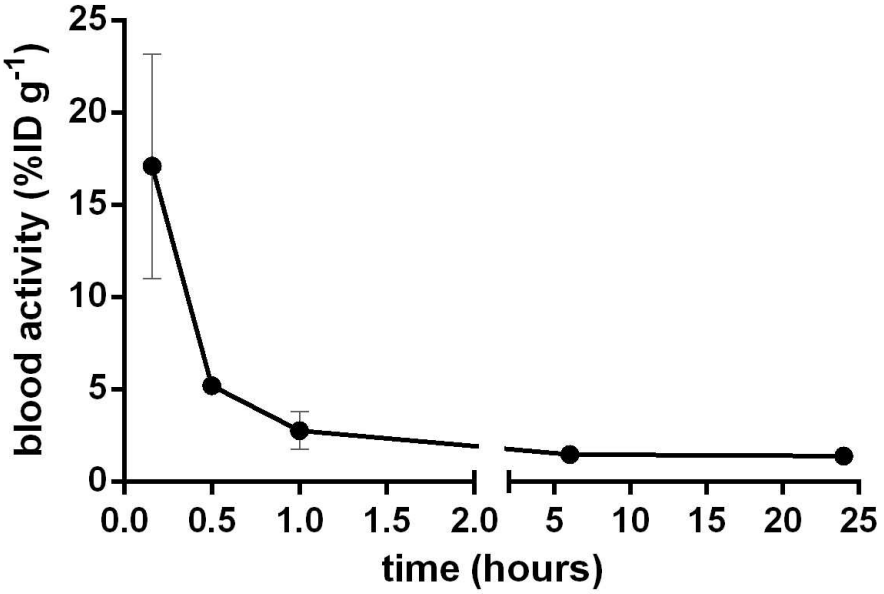

Figure 4: Blood activity at various time points of the $scFv_{anti\text{-}LIBS}$-^{64}CuMeCOSar as % injected dose per body weight (g) after intravenous injection of the radiotracer, n=3. Over 90% of the radiotacer is eliminated with 30 mins.

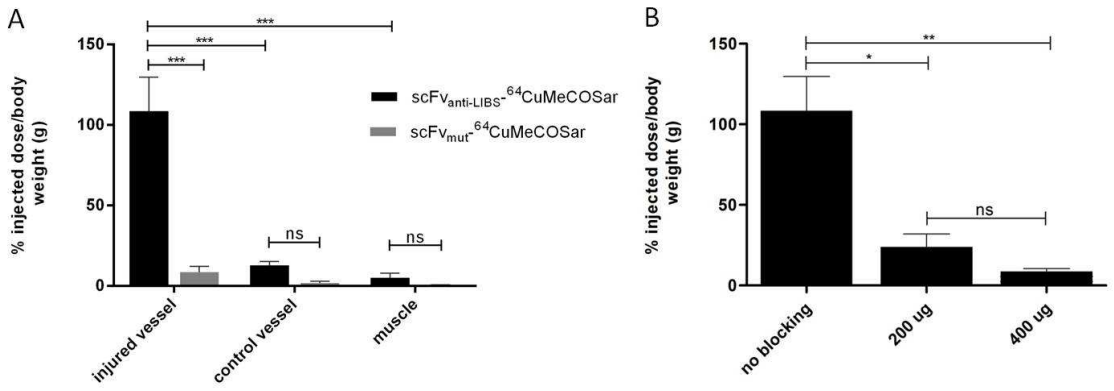

Figure 5: A) Uptake of scFv$_{anti-LIBS}$-^{64}CuMeCOSar (black bar) and scFv$_{mut}$-^{64}CuMeCOSar (grey bar) in the injured vessel compared to the non-injured vessel and the muscle. B) Blocking of scFv$_{anti-LIBS}$-^{64}CuMeCOSar uptake in an *in vivo* model of mouse carotid artery thrombosis with 200 µg and 400 µg of non-radioactive scFv$_{anti-LIBS}$, given 30 min before radiotracer injection. Data are given as % injected dose per body weight (g) 90 min after tracer injection (*/p=0.01, **/p=0.005, ***/p=0.001, ns = non-significant, n=6).

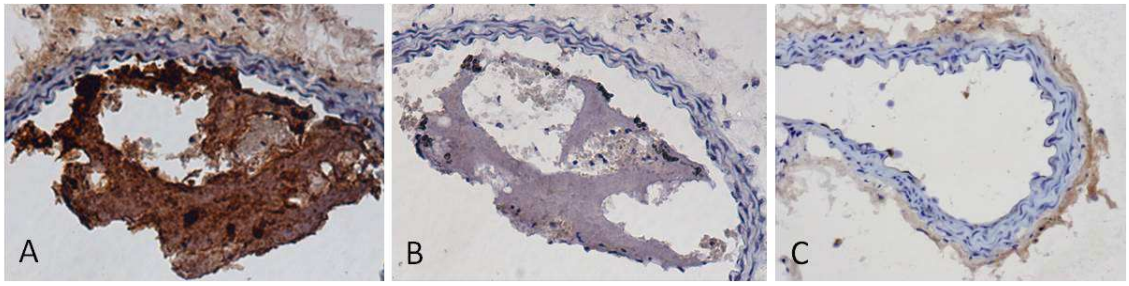

Figure 6: Immunohistochemistry for activated platelets. Injured and non-injured vessel sections were stained with anti-human CD 41 and detected with a secondary peroxidase antibody (A, C) or PBS as negative control (omit primary antibody control, B). Positive (brown) staining for platelets is observed in the injured vessel (A) and is absent in the control staining (B) or the non-injured vessel (C). Representative pictures are shown.

Table 1: Uptake as measured by micro PET/CT analysis. The estimated activities from regions of interest (ROI) in the injured vessel, control vessel and control soft tissue control are shown.

Tissue	$scFv_{anti\text{-}LIBS}$-^{64}CuMeCOSar			$scFv_{mut}$-^{64}CuMeCOSar		
Injury vessel	3.5****	±	0.34	0.92	±	0.17
Control vessel	0.25	±	0.17	0.19	±	0.16
Soft tissue	0.15	±	0.094	0.01	±	0.004

Data are SUV expressed as mean ± SD.

(*/p=0.01, **/p=0.005, ***/p=0.001, ****/p=0.0001, n=6)

Table 2: Biodistribution of $scFv_{anti\text{-}LIBS}$-^{64}CuMeCOSar in BALB/c mice 90 mins after tracer injection.

Tissue	90 min (n=3)		
blood	1.87	±	0.92
liver	12.90	±	10.29
kidney r	26.89	±	12.73
kidney l	29.17	±	14.04
heart	0.45	±	0.20
lung	1.77	±	0.83
vessel	0.51	±	0.33
spleen	10.90	±	9.74
muscle	0.23	±	0.10
bladder	32.38	±	13.49

Data are %ID/g expressed as mean ± SD.

Acknowledgments

This work was funded by the National Health and Medical Research Council (NHMRC), Grants 1029249, 1017670 and 1011418 as well as the Australian Research Council (P.S.D.). K.Al. is supported by the German Research Foundation (Al 1521/1-1). K.Ar. is supported by the NHMRC and the National Heart Foundation (586740). K.P. is supported by an Australian Research Council Future Fellowship (FT0992210). C.E.H. is supported by a NHMRC Career Development Fellowship (472668). This research was undertaken using equipment provided by Monash Biomedical Imaging, Monash University as part of the Victorian Biomedical Imaging Capability (Victorian Government). The work was also supported in part by the Victorian Government's Operational Infrastructure Support Program, Victoria's Science Agenda Strategic Project Fund and the PET Solid Target Laboratory, an ANSTO-Austin-LICR Cyclotron Partnership.

REFERENCES

(1) Go, A. S.; Mozaffarian, D.; Roger, V. L.; Benjamin, E. J.; Berry, J. D.; Borden, W. B.; Bravata, D. M.; Dai, S.; Ford, E. S.; Fox, C. S.; Franco, S.; Fullerton, H. J.; Gillespie, C.; Hailpern, S. M.; Heit, J. A.; Howard, V. J.; Huffman, M. D.; Kissela, B. M.; Kittner, S. J.; Lackland, D. T.; Lichtman, J. H.; Lisabeth, L. D.; Magid, D.; Marcus, G. M.; Marelli, A.; Matchar, D. B.; McGuire, D. K.; Mohler, E. R.; Moy, C. S.; Mussolino, M. E.; Nichol, G.; Paynter, N. P.; Schreiner, P. J.; Sorlie, P. D.; Stein, J.; Turan, T. N.; Virani, S. S.; Wong, N. D.; Woo, D.; Turner, M. B.; on behalf of the American Heart Association Statistics Committee and Stroke Statistics Subcommittee. Heart Disease and Stroke Statistics--2013 Update: a Report From the American Heart Association. *Circulation* **2013**, *127*, e6–e245.

(2) Hansson, G. K. Inflammation, Atherosclerosis, and Coronary Artery Disease. *N. Engl. J. Med.* **2005**, *352*, 1685–1695.

(3) Gawaz, M.; Langer, H.; May, A. E. Platelets in Inflammation and Atherogenesis. *J. Clin. Invest.* **2005**, *115*, 3378–3384.

(4) Finn, A. V.; Nakano, M.; Narula, J.; Kolodgie, F. D.; Virmani, R. Concept of Vulnerable/Unstable Plaque. *Arterioscler. Thromb. Vasc. Biol.* **2010**, *30*, 1282–1292.

(5) Wang, X.; Hagemeyer, C. E.; Hohmann, J. D.; Leitner, E.; Armstrong, P. C.; Jia, F.; Olschewski, M.; Needles, A.; Peter, K.; Ahrens, I. Novel Single-Chain Antibody-Targeted Microbubbles for Molecular Ultrasound Imaging of Thrombosis: Validation of a Unique Noninvasive Method for Rapid and Sensitive Detection of Thrombi and Monitoring of Success or Failure of Thrombolysis in Mice. *Circulation* **2012**, *125*, 3117–3126.

(6) von zur Muhlen, C.; Sibson, N. R.; Peter, K.; Campbell, S. J.; Wilainam, P.; Grau, G. E.; Bode, C.; Choudhury, R. P.; Anthony, D. C. A Contrast Agent Recognizing Activated Platelets Reveals Murine Cerebral Malaria Pathology Undetectable by Conventional MRI. *J. Clin. Invest.* **2008**, *118*, 1198–1207.

(7) von zur Muhlen, C.; von Elverfeldt, D.; Moeller, J. A.; Choudhury, R. P.; Paul, D.; Hagemeyer, C. E.; Olschewski, M.; Becker, A.; Neudorfer, I.; Bassler, N.; Schwarz, M.; Bode, C.; Peter, K. Magnetic Resonance Imaging Contrast Agent Targeted Toward Activated Platelets Allows in Vivo Detection of Thrombosis and Monitoring of Thrombolysis. *Circulation* **2008**, *118*, 258–267.

(8) Stoll, P.; Bassler, N.; Hagemeyer, C. E.; Eisenhardt, S. U.; Chen, Y. C.; Schmidt, R.; Schwarz, M.; Ahrens, I.; Katagiri, Y.; Pannen, B.; Bode, C.; Peter, K. Targeting

Ligand-Induced Binding Sites on GPIIb/IIIa via Single-Chain Antibody Allows Effective Anticoagulation Without Bleeding Time Prolongation. *Arterioscler. Thromb. Vasc. Biol.* **2007**, *27*, 1206–1212.

(9) Hagemeyer, C. E.; Peter, K. Targeting the Platelet Integrin GPIIb/IIIa. *Curr. Pharm. Des.* **2010**, *16*, 4119–4133.

(10) Blower, P. J.; Lewis, J. S.; Zweit, J. Copper Radionuclides and Radiopharmaceuticals in Nuclear Medicine. *Nucl. Med. Biol.* **1996**, *23*, 957–980.

(11) Shokeen, M.; Anderson, C. J. Molecular Imaging of Cancer with Copper-64 Radiopharmaceuticals and Positron Emission Tomography (PET). *Acc. Chem. Res.* **2009**, *42*, 832–841.

(12) Wadas, T. J.; Wong, E. H.; Weisman, G. R.; Anderson, C. J. Coordinating Radiometals of Copper, Gallium, Indium, Yttrium, and Zirconium for PET and SPECT Imaging of Disease. *Chem. Rev.* **2010**, *110*, 2858–2902.

(13) Smith, S. V. Molecular Imaging with Copper-64. *J. Inorg. Biochem.* **2004**, *98*, 1874–1901.

(14) Vavere, A. L.; Butch, E. R.; Dearling, J. L. J.; Packard, A. B.; Navid, F.; Shulkin, B. L.; Barfield, R. C.; Snyder, S. E. 64Cu-P-NH2-Bn-DOTA-hu14.18K322A, a PET Radiotracer Targeting Neuroblastoma and Melanoma. *J. Nucl. Med.* **2012**, *53*, 1772–1778.

(15) Bryan, J. N.; Jia, F.; Mohsin, H.; Sivaguru, G.; Anderson, C. J.; Miller, W. H.; Henry, C. J.; Lewis, M. R. Monoclonal Antibodies for Copper-64 PET Dosimetry and Radioimmunotherapy. *Cancer Biol. Ther.* **2011**, *11*, 1001–1007.

(16) Ma, M. T.; Karas, J. A.; White, J. M.; Scanlon, D.; Donnelly, P. S. A New Bifunctional Chelator for Copper Radiopharmaceuticals: a Cage Amine Ligand with a Carboxylate Functional Group for Conjugation to Peptides. *Chem. Commun.* **2009**, *14*, 3237–3239.

(17) Di Bartolo, N.; Sargeson, A. M.; Smith, S. V. New 64Cu PET Imaging Agents for Personalised Medicine and Drug Development Using the Hexa-Aza Cage, SarAr. *Org. Biomol. Chem.* **2006**, *4*, 3350–3357.

(18) Lears, K. A.; Ferdani, R.; Liang, K.; Zheleznyak, A.; Andrews, R.; Sherman, C. D.; Achilefu, S.; Anderson, C. J.; Rogers, B. E. In Vitro and in Vivo Evaluation of 64Cu-Labeled SarAr-Bombesin Analogs in Gastrin-Releasing Peptide Receptor-Expressing Prostate Cancer. *J. Nucl. Med.* **2011**, *52*, 470–477.

(19) Cai, H.; Fissekis, J.; Conti, P. S. Synthesis of a Novel Bifunctional Chelator

AmBaSar Based on Sarcophagine for Peptide Conjugation and ^{64}Cu Radiolabelling. *Dalton Trans.* **2009**, 5395–5400.

(20) Sargeson, A. M. The Potential for the Cage Complexes in Biology. *Coord. Chem. Rev.* **1996**, *151*, 89–114.

(21) Cooper, M. S.; Ma, M. T.; Sunassee, K.; Shaw, K. P.; Williams, J. D.; Paul, R. L.; Donnelly, P. S.; Blower, P. J. Comparison of ^{64}Cu-Complexing Bifunctional Chelators for Radioimmunoconjugation: Labeling Efficiency, Specific Activity, and in Vitro/in Vivo Stability. *Bioconjugate Chem.* **2012**, *23*, 1029–1039.

(22) Lewis, M. R.; Kao, J. Y.; Anderson, A. L.; Shively, J. E.; Raubitschek, A. An Improved Method for Conjugating Monoclonal Antibodies with N-Hydroxysulfosuccinimidyl DOTA. *Bioconjugate Chem.* **2001**, *12*, 320–324.

(23) Alt, K.; Wiehr, S.; Ehrlichmann, W.; Reischl, G.; Wolf, P.; Pichler, B. J.; Elsässer-Beile, U.; Bühler, P. High-Resolution Animal PET Imaging of Prostate Cancer Xenografts with Three Different 64Cu-Labeled Antibodies Against Native Cell-Adherent PSMA. *Prostate* **2010**, *70*, 1413–1421.

(24) Semple, J. W.; Italiano, J. E.; Freedman, J. Platelets and the Immune Continuum. *Nat. Rev. Immunol.* **2011**, *11*, 264–274.

(25) Olafsen, T.; Wu, A. M. Antibody Vectors for Imaging. *Semin. Nucl. Med.* **2010**, *40*, 167–181.

(26) Voss, S. D.; Smith, S. V.; DiBartolo, N.; McIntosh, L. J.; Cyr, E. M.; Bonab, A. A.; Dearling, J. L. J.; Carter, E. A.; Fischman, A. J.; Treves, S. T.; Gillies, S. D.; Sargeson, A. M.; Huston, J. S.; Packard, A. B. Positron Emission Tomography (PET) Imaging of Neuroblastoma and Melanoma with 64Cu-SarAr Immunoconjugates. *Proc. Natl. Acad. Sci. U.S.A.* **2007**, *104*, 17489–17493.

(27) Paterson, B. M.; Roselt, P.; Denoyer, D.; Cullinane, C.; Binns, D.; Noonan, W.; Jeffery, C. M.; Price, R. I.; White, J. M.; Hicks, R. J.; Donnelly, P. S. PET Imaging of Tumours with a ^{64}Cu Labeled Macrobicyclic Cage Amine Ligand Tethered to Tyr^3-Octreotate. *Dalton Trans.* **2014**, *43*, 1386–1396.

(28) Wu, A. M.; Senter, P. D. Arming Antibodies: Prospects and Challenges for Immunoconjugates. *Nat. Biotechnol.* **2005**, *23*, 1137–1146.

(29) Kenanova, V.; Wu, A. M. Tailoring Antibodies for Radionuclide Delivery. *Expert Opin. Drug. Deliv.* **2006**, *3*, 53–70.

(30) Olafsen, T.; Kenanova, V. E.; Wu, A. M. Tunable Pharmacokinetics: Modifying the in Vivo Half-Life of Antibodies by Directed Mutagenesis of the Fc Fragment. *Nat.*

Protoc. **2006**, *1*, 2048–2060.

(31) Holliger, P.; Hudson, P. J. Engineered Antibody Fragments and the Rise of Single Domains. *Nat. Biotechnol.* **2005**, *23*, 1126–1136.

(32) Langer, H. F.; Haubner, R.; Pichler, B. J.; Gawaz, M. Radionuclide Imaging: a Molecular Key to the Atherosclerotic Plaque. *J. Am. Coll. Cardiol.* **2008**, *52*, 1–12.

(33) Laitinen, I.; Saraste, A.; Weidl, E.; Poethko, T.; Weber, A. W.; Nekolla, S. G.; Leppänen, P.; Ylä-Herttuala, S.; Hölzlwimmer, G.; Walch, A.; Esposito, I.; Wester, H.-J.; Knuuti, J.; Schwaiger, M. Evaluation of Alphavbeta3 Integrin-Targeted Positron Emission Tomography Tracer 18F-Galacto-RGD for Imaging of Vascular Inflammation in Atherosclerotic Mice. *Circ. Cardiovasc. Imaging* **2009**, *2*, 331–338.

(34) Bassler, N.; Loeffler, C.; Mangin, P.; Yuan, Y.; Schwarz, M.; Hagemeyer, C. E.; Eisenhardt, S. U.; Ahrens, I.; Bode, C.; Jackson, S. P.; Peter, K. A Mechanistic Model for Paradoxical Platelet Activation by Ligand-Mimetic alphaIIb Beta3 (GPIIb/IIIa) Antagonists. *Arterioscler. Thromb. Vasc. Biol.* **2007**, *27*, e9–e15.

(35) Du, X. P. X.; Plow, E. F. E.; Frelinger, A. L. A.; O'Toole, T. E. T.; Loftus, J. C. J.; Ginsberg, M. H. M. Ligands "Activate" Integrin Alpha IIb Beta 3 (Platelet GPIIb-IIIa). *Cell* **1991**, *65*, 409–416.

(36) Bass, L. A.; Wang, M.; Welch, M. J.; Anderson, C. J. In Vivo Transchelation of Copper-64 From TETA-Octreotide to Superoxide Dismutase in Rat Liver. *Bioconjugate Chem.* **2000**, *11*, 527–532.

(37) Boswell, C. A.; Sun, X.; Niu, W.; Weisman, G. R.; Wong, E. H.; Rheingold, A. L.; Anderson, C. J. Comparative in Vivo Stability of Copper-64-Labeled Cross-Bridged and Conventional Tetraazamacrocyclic Complexes. *J. Med. Chem.* **2004**, *47*, 1465–1474.

(38) Schwarz, M.; Meade, G.; Stoll, P.; Ylanne, J.; Bassler, N.; Chen, Y. C.; Hagemeyer, C. E.; Ahrens, I.; Moran, N.; Kenny, D.; Fitzgerald, D.; Bode, C.; Peter, K. Conformation-Specific Blockade of the Integrin GPIIb/IIIa: a Novel Antiplatelet Strategy That Selectively Targets Activated Platelets. *Circ. Res.* **2006**, *99*, 25–33.

(39) Poniger, S. S.; Tochon-Danguy, H. J. Automated Production of I and Cu Using IBA Terimo and Pinctada Metal Electroplating and Processing Modules. *AIP Conf. Proc.* **2012**, *1509*, 114–119.